



Organophosphorus Compound Formation Through the Oxidation of Reduced Oxidation State Phosphorus Compounds on the Hadean Earth

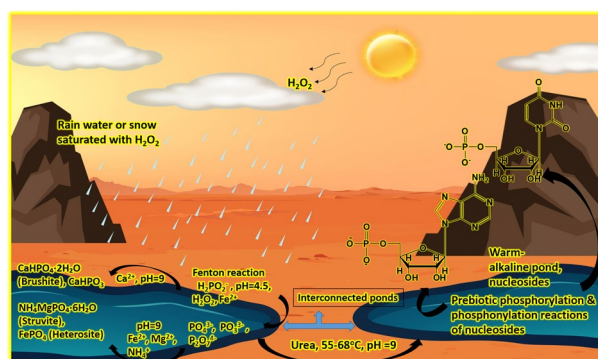
Maheen Gull¹ · Tian Feng¹ · Joe Bracegirdle² · Heather Abbott-Lyon³ · Matthew A. Pasek¹

Received: 1 September 2022 / Accepted: 16 December 2022 / Published online: 28 December 2022
 © The Author(s), under exclusive licence to Springer Science+Business Media, LLC, part of Springer Nature 2022

Abstract

Reduced oxidation state phosphorus compounds may have been brought to the early Earth via meteorites or could have formed through geologic processes. These compounds could have played a role in the origin of biological phosphorus (P, hereafter) compounds. Reduced oxidation state P compounds are generally more soluble in water and are more reactive than orthophosphate and its associated minerals. However, to date no facile routes to generate C–O–P type compounds using reduced oxidation state P compounds have been reported under prebiotic conditions. In this study, we investigate the reactions between reduced oxidation state P compounds—and their oxidized products generated via Fenton reactions—with the nucleosides uridine and adenosine. The inorganic P compounds generated via Fenton chemistry readily react with nucleosides to produce organophosphites and organophosphates, including phosphate diesters via *one-pot syntheses*. The reactions were facilitated by NH_4^+ ions and urea as a condensation agent. We also present the results of the plausible stability of the organic compounds such as adenosine in an environment containing an abundance of H_2O_2 . Such results have direct implications on finding organic compounds in Martian environments and other rocky planets (including early Earth) that were richer in H_2O_2 than O_2 . Finally, we also suggest a route for the sink of these inorganic P compounds, as a part of a plausible natural P cycle and show the possible formation of secondary phosphate minerals such as struvite and brushite on the early Earth.

Graphical Abstract



Keywords Origin of life · Nucleoside phosphorylation · Reduced oxidation phosphorus compounds · Fenton chemistry · Chemical evolution · Macromolecules

Abbreviations

P	Phosphorus
MS	Mass spectrometry
LCMS	Liquid chromatography-mass spectrometry

Handling Editor: Ulrich Muller.

Extended author information available on the last page of the article

PAA	Phosphonoacetic acid
U-P-U and Ad-P-Ad	Phosphate diester of uridine and adenosine
5'-UMP	Uridine-5-monophosphate
2'-UMP	Uridine-2-monophosphate
3'-UMP	Uridine-3-monophosphate
5'-AMP	Adenosine-5-monophosphate
2'-AMP	Adenosine-2-monophosphate
3'-AMP	Adenosine-3-monophosphate

Introduction

RNA-based life likely preceded modern DNA-based life (Gilbert 1986; Hud et al. 2013). The formation of RNA requires the element P, which makes up the phosphate backbone of the nucleic acid. Hence, P chemistry must have played a central role in the chemical evolution of RNA biochemistry. On the early Earth, P is presumed to have occurred mainly as phosphates, most likely as orthophosphate minerals (Schwartz 2006). Divalent cations such as Mg^{2+} and Ca^{2+} were likely ubiquitous in the Hadean ocean and caused phosphate to precipitate out in mineral form, including as apatites ($\text{Ca}_5(\text{PO}_4)_3(\text{F}, \text{Cl}, \text{OH})$) (Keefe and Miller 1995) and other minerals such as whitlockite ($\text{Ca}_9(\text{Mg}, \text{Fe})(\text{PO}_4)_6\text{PO}_3\text{OH}$), and brushite ($\text{CaHPO}_4 \cdot 2\text{H}_2\text{O}$) (Arrhenius et al. 1997; Hazen et al. 2008). These phosphate minerals are poorly soluble in water and have low reactivity toward organics, as discussed elsewhere (Pasek and Kee 2011; Gull 2014; Pasek et al. 2017).

Water is generally accepted as the most prebiotically relevant solvent for chemistry on the early Earth due to its simplicity and abundance in the universe, and we expect aqueous prebiotic reactions to dominate, including production of prebiotic phosphorylated compounds in water. However, phosphorylation reactions are condensation reactions and their formation in aqueous environments is problematic as phosphorylation thermodynamics in water are endergonic, requiring energy for the condensation reaction to proceed (Pasek 2008, 2019). Hence, the prebiotic synthesis of biological compounds containing P has long been a challenging question in astrobiology (Lohrmann and Orgel 1968). An alternative route to address prebiotic reactions with P is the use of non-aqueous solvents (Schoffstall 1976; Saladino et al. 2012; Gull et al. 2014, 2017; Burcar et al. 2016, 2019), but the plausible presence of such systems as solvents on the early Earth, much less their widespread occurrence, has been questioned. Reactions within these solvents may not be a realistic prebiotic scenario, though there may exist routes to forming these solvents in the ratios needed to perform the chemistry (Lago et al. 2020).

Another proposed route is the use of reduced oxidation state P compounds (Gulick 1955). These reduced oxidation

state P compounds can be 10^3 – 10^6 times more soluble in water as compared to orthophosphates in the presence of divalent cations (Pasek and Kee 2011; Pasek et al. 2017). The possibility that these P compounds may have been relevant to early Earth geology is further supported by discoveries such as the occurrence of phosphonic acids in the Murchison meteorite (Cooper et al. 1992) and phosphites in early Archean marine carbonates (Pasek et al. 2013). Another noteworthy source of reduced oxidation state P compounds species could be extraterrestrial impacts that could have triggered the origin of life on the early Earth (Simonson et al. 1998; Simonson and Glass 2004; Pasek and Laurretta 2005; Pasek et al. 2013).

The mineral schreibersite, $(\text{Fe}, \text{Ni})_3\text{P}$, releases water-soluble P species upon corrosion in water including the ion phosphite (Pasek and Laurretta 2005; Pasek et al. 2007). Aqueous reactions of schreibersite can yield organophosphates such as glycerol phosphate and even nucleotides of adenosine and uridine by simple mixing and heating at low temperatures (Pasek et al. 2013; Gull et al. 2015). Such chemical reactions are significant as these generate building blocks of DNA, RNA (nucleotides), and cell membranes (glycerol phosphate), though the reported yields are low (Pasek et al. 2013; Gull et al. 2015).

Reduced oxidation state P compounds can oxidize in the presence of ultraviolet light and $\text{H}_2\text{S}/\text{HS}^-$, to form PO_4^{3-} via a thiophosphate intermediate (Ritson et al. 2020) or alternatively the oxidation of phosphite or hypophosphite with peroxides in the presence of a Fe^{2+} catalyst also generates phosphates (Pasek et al. 2008). The latter mimics a plausible prebiotic route for the oxidation of phosphite (HPO_3^{2-} or hypophosphite (H_2PO_2^-) aqueous solutions by Fenton reaction, which generates reactive free radicals such as $\cdot\text{OH}$ and $\cdot\text{OOH}$ in the presence catalytic iron (Pasek et al. 2008). These hydroxyl radicals oxidize reduced P compounds by cleaving the H-P bond to form phosphite radicals that can recombine to phosphate (PO_4^{3-}) as well as condensed phosphates including pyrophosphate ($\text{HP}_2\text{O}_7^{3-}$), triphosphate ($\text{H}_3\text{P}_3\text{O}_{10}^{2-}$), and trimetaphosphate ($\text{P}_3\text{O}_9^{3-}$). The Fenton reaction requires H_2O_2 , which would be a strong oxidant in anoxic environments (Liang et al. 2006).

The presence of H_2O_2 in the Martian atmosphere (Blankenship and Hartman 1998; Raymond and Blankenship 2008) supports the idea that the oxidation of iron by the photochemically generated H_2O_2 over the past billion years could have given rise to the present, likely thin oxidized Martian surface (Olson 1970; Liang et al. 2006). Hydrogen peroxide may have been abundant on the early rocky planets including Earth, with routes to its possible formation including the photolysis of atmospheric water (Levine et al. 1979; Ślesak et al. 2012) or ice (Liang et al. 2006). It is possible that dry, cold, and low-oxygen conditions could have facilitated the generation of H_2O_2 via

chemical processes involving photolytic conversion of H_2O in Archean atmospheres (Padan 1979; Liang et al. 2006; Lalonde and Konhauser 2015). This may have included photolysis of water ice, potentially producing copious amounts of H_2O_2 that could have been part of glaciers during “Snowball Earth” events (Liang et al. 2006). Alternatively, H_2O_2 has also been postulated to be generated through abiotic pathway in the Archean through a process involving the abrasion of quartz surfaces, followed by the generation of certain surface bound radicals that oxidize H_2O to H_2O_2 and O_2 (He et al. 2021).

Therefore, the generation of phosphates (including polyphosphates) from reduced P compounds on the early Earth would likely have occurred if oxidants mixed with water bearing both reduced oxidation state P source and dissolved iron (Pasek et al. 2008). However, it is unknown whether a reaction mixture of reduced P compounds and their oxidized P products as a whole could react with organic compounds, including nucleosides and organic alcohols, to form organic phosphates and phosphites. Additionally, the survivability of organic molecules in the presence of excess H_2O_2 on the early Earth is unknown. Could C–O–P bond formation possibly have existed in an environment saturated with H_2O_2 ?

We investigate here the phosphorylation and phosphorylation reactions of uridine and adenosine with phosphate, phosphite, and polyphosphates generated through Fenton chemistry. The overall process is divided into two main phases: phase (1) generation of phosphite, phosphate, and polyphosphates from the reaction of H_2O_2 with hypophosphite and Fe^{2+} ions at pH=4.5, 22 °C–25 °C, followed by quenching with a base (either NaOH or NH_4OH , which liberates P from the iron oxyhydroxides and allows for NMR analysis) and phase (2) reaction of inorganic P compounds generated via Fenton chemistry with nucleosides at 55 °C–68 °C, around pH=9–9.5, promoted by ammonium ions and urea. The former phase mimics the general conditions believed to exist on the early Earth (and is the pH of a Fenton solution, controlled by the pH of the weak acids FeCl_2 and H_2O_2), while the latter phase mimics a prebiotic ‘mildly hot drying alkaline spring/pool’. This work is buttressed by a study of the stability of adenosine in a solution saturated with H_2O_2 , wherein the decomposition rates of adenosine in such environments were investigated over time.

Furthermore, considering the prebiotic significance, ubiquity, and relevance of Mg^{2+} and Ca^{2+} ions on the early Earth (Keefe and Miller 1995; Arrhenius et al. 1997; Hazen et al. 2008; Holm 2012; Gull et al. 2020) the effects of these ions were also studied on the solution chemistry of the Fenton reaction. We investigate the addition of Ca^{2+} or Mg^{2+} to the Fenton reaction solution, focusing on the precipitation of phosphate minerals including brushite and struvite (Burcar et al. 2016, 2019).

Materials and Methods

Materials for organophosphorus compound production experiments included: sodium hypophosphite hydrate ($\text{NaH}_2\text{PO}_2 \cdot \text{H}_2\text{O}$, 98%), ethylenediaminetetraacetic acid powder (EDTA, 99.5%), 2'-deoxyriboadenosine, standard compounds (uridine-5-monophosphate (5'-UMP), adenosine-5-monophosphate (5'-AMP), 2',3'-cyclic AMP and 3',5'-cyclic AMP were purchased from Sigma Aldrich while sodium hydroxide (NaOH, 98.5%), sodium pyrophosphate ($\text{Na}_4\text{P}_2\text{O}_7$, 99%), phosphorous acid (H_3PO_3 , 98%) sodium phosphite (Na_2HPO_3), adenosine ($\text{C}_{10}\text{H}_{13}\text{N}_5\text{O}_4$, 98%), and deuterium oxide (D_2O , 99.8% atom %D) were from Acros Organic. Ammonium hydroxide (NH_4OH , 25% solution in water), synthetic brushite ($\text{CaHPO}_4 \cdot 2\text{H}_2\text{O}$), calcium chloride (CaCl_2 , 98%), and ferrous chloride tetrahydrate ($\text{FeCl}_2 \cdot 4\text{H}_2\text{O}$, 98%) were purchased from Alfa Aesar. Uridine ($\text{C}_9\text{H}_{12}\text{N}_2\text{O}_6$, 98%) was from TCI and hydrogen peroxide (H_2O_2 , 30% v/v) was from Fisher Scientific. Vivianite ($\text{Fe}_3(\text{PO}_4)_2 \cdot 8\text{H}_2\text{O}$), and apatite ($\text{Ca}_5(\text{PO}_4)_3(\text{F}, \text{Cl}, \text{OH})$) were purchased from Amazon.

Deionized water was obtained using a Barnstead (Dubuque, IA, USA) NANO pure® Diamond Analytical combined reverse osmosis-deionization system as also previously reported (Pasek et al. 2013). FeHPO_3 was prepared by mixing the equimolar solutions of $\text{FeCl}_2 \cdot 4\text{H}_2\text{O}$ and H_3PO_3 (0.1 M each) and on mixing brownish precipitates were separated which were filtered, dried, and stored for future use.

For ^{31}P -NMR analysis, the reaction samples were analyzed on a 400-MHz Varian Unity Inova NMR operating at 161.9 MHz in both H-coupled and H-decoupled modes. The width of the spectrum was 200 ppm, and the running temperature was 25 °C. Phosphorylation and phosphorylation products (which will be collectively referred to as C–O–P type compounds, unless mentioned otherwise) were quantified by peak integration method as previously reported (Pasek et al. 2013; Gull et al. 2014, 2015, 2017) and also using an internal standard (see SI). The instrumentation details and the parameters for the ^{31}P -NMR have been reported in our previous studies (Pasek et al. 2013; Gull et al. 2014, 2015, 2017). ^{13}C -NMR was performed in H-decoupled mode using D_2O as a solvent and with other conditions being the same as reported previously.

Mass spectrometry (MS) analyses were done in negative ion mode on a 6130 Single Quadrupole Mass Spectrometer (Agilent, Santa Clara, CA, USA) attached to an Agilent 1200 HPLC by direct injection, and deionized water was used as a solvent as reported previously (Gull et al. 2020).

Laser Raman spectroscopy analysis were performed to study the mineralogy of the reaction. An Enwave Opt. Inc. (Model No. EZI-785-A2) Laser Raman Spectroscopy

was used to determine the precipitates formed as a result of adding CaCl_2 or MgCl_2 solutions to the quenched Fenton solution and as described in Sect. “**Oxidation of Reduced P Compounds via Fenton Chemistry**”. The Raman microscope was a Leica DM 300 microscope that was equipped with three objective lenses ($\times 4/0.1 \text{ NA}$, $\times 10/0.25 \text{ NA}$ and $\times 40/0.65 \text{ NA}$). Every mineral sample analysis was performed between 1 min by using a 785 nm laser (at 300 mW) as reported previously (Pasek and Pasek 2018) and Crystal Sleuth software (Laetsch and Downs 2006) was used to determine the sample product and was compared with the data provided in RRUFF database (Lafuente et al. 2015; Feng et al. 2019).

For powder XRD analysis, a BTX-402 benchtop XRD was also utilized to study the formation of products also analyzed by laser Raman spectroscopy. A calibrated ion chamber, Ludium Model 9–3 Radiation Ion Chamber, was received for the measurements which measured radiation level counting range of 0 to 2000 $\mu\text{Sv}/\text{Hr}$. The scan rate was 0.054 ($^\circ/\text{s}$) under 30.5 kV voltage and 0.33 mA current intensity.

LCMS analyses were carried out on an Agilent 6540 QTOF LC/MS equipped with a Kinetex Polar C18 column (2.6 μm , 100 \AA , 100 \times 4.6 mm; 0.5 mL/min). For adenosine quantification, the mobile phase was 100% H_2O (0.1% formic acid) for 2 min, followed by a linear gradient to 20% acetonitrile/ H_2O (0.1% formic acid) over 3 min and then an isocratic hold for 4 min, to give adenosine retention ($\text{RT} = 6.75 \text{ min}$). The protonated molecule at m/z 268.1053 was then extracted and integrated using the Agilent MassHunter Qualitative Analysis program to give the relative area which was then compared to a standard curve to calculate the relative quantity of adenosine in the solution.

Reactions (detailed below) were carried out in the following sequence (1) forming a Fenton solution with reduced P compounds as described previously (Pasek et al. 2008), (2) neutralizing solutions with OH^- to quench further oxidation and precipitate iron compounds and filtration of the reaction mixture and storing for further use, (3) adding organic substrates to examine phosphorylation/phosphorylation extent, (4) analyzing the C–O–P type compounds by ^{31}P nuclear magnetic resonance (^{31}P -NMR) spectroscopy and mass spectrometry (MS), (5) using X-ray diffractometry (XRD) and Raman spectroscopy for studying the inorganic Fe–P products with additions of Ca^{2+} and Mg^{2+} solutions of the Fenton mixture were and finally, (6) monitoring by ^{13}C -NMR and quantified by LCMS the decomposition rates of adenosine in water with H_2O_2 and Fe^{2+} , as an investigation of the durability of organic compounds in the Fenton reaction.

Oxidation of Reduced P Compounds Via Fenton Chemistry

The starting material for Fenton reaction chemistry of reduced P compounds was sodium hypophosphite (NaH_2PO_2) and its ^{31}P -NMR analysis revealed no other P peaks as impurities (SI Fig. S-1a). The Fenton reactions were generated by the method previously reported (Pasek et al. 2008): aqueous solutions were prepared by mixing 0.2 M of both hypophosphite (H_2PO_2^-) and $\text{FeCl}_2 \cdot 4\text{H}_2\text{O}$ (equal volumes, 0.1 M total of each). The total volume of the solution was 20 mL (i.e., 10 mL for each of the above-mentioned solution). To this mixture, 15 mL of 0.50 M H_2O_2 was added dropwise, although various concentrations of H_2O_2 were employed to observe the extent of conversion of the reduced oxidation state P compounds by the Fenton reactor as previously (Pasek et al. 2008). The pH of the reaction mixture was 4.5. The reaction vial was covered and was allowed to stir at room temperature for 10–24 h and was subsequently quenched and titrated by 20% ammonium hydroxide (NH_4OH) or 0.1 M NaOH solution (about 15 mL) to a pH of 9.5. Thick orange-brown precipitates were formed, likely insoluble Fe^{3+} precipitating as Fe(III)(O,OH)_x compounds. The resulting solution mixture was filtered and stored for further use. This filtrate of the above-mentioned Fenton reaction was labeled as inorganic P Fenton solution (IPF solution hereafter). Various concentrations of the sample solutions are given in detail (SI, Table S-1). Fenton reactions of the reduced oxidation state P compounds were also carried out under anaerobic conditions (SI, Fig. S-1b). The details of the various solution concentrations, reaction conditions are discussed in the SI (Tables S-1–3).

Phosphonylation and Phosphorylation Reactions

Phosphonylation and phosphorylation reactions with the Fenton solution proceeded by taking 7 mL of IPF solution in a clean and unsealed glass vial, to which 0.65 g of nucleoside and 0.50 g of urea were added. In some experiments, 0.50 g of urea or an additional 2 mL of concentrated NH_4OH solution (or both) were added, as possible condensation agents. The unsealed reaction vial was then allowed to heat at 55 $^\circ\text{C}$ –68 $^\circ\text{C}$ from 5 h to 6 days (see SI, Tables S-1–3). The reaction mixture was kept unsealed to promote subsequent evaporation of the water from the solution.

After 5 h to 6 days, the dried sample was cooled down to room temperature and was rehydrated with 5 mL DI water. The dried reaction sample was mixed and stirred until a clear solution was formed, which was filtered and then transferred to a watch glass followed by air-drying at room temperature. The air-dried room temperature sample was then rehydrated with a 2 mL D_2O (75%) and DI water (25%) solution (or only DI water in the case of analysis for

MS) and was centrifuged. The total volume of the solution was 2 mL. About 400 μL of the sample solution was transferred to a clean NMR tube and analyzed by ^{31}P -NMR.

A few experiments were also attempted with unquenched Fenton solutions in which uridine was directly heated with the Fenton solution without quenching with a base. Similar protocols were used to generate the Fenton solution (Sect. “[Oxidation of Reduced P Compounds via Fenton Chemistry](#)”), but quenching was not followed with any base (NaOH or NH_4OH). About 7 mL of the Fenton solution ($\text{pH}=4.5$) was taken into a clean glass vial and the same weighed amounts of organics (0.65 g nucleoside and 0.50 g of urea) were added as mentioned above. The reaction sample was heated to dryness at 65°C for 2–3 days. After the completion of the reaction, the dried mixture was treated with 0.1 M NaOH solution to precipitate out Fe^{3+} for better analysis through ^{31}P -NMR. The mixture then followed the same protocol and was analyzed by ^{31}P -NMR.

A set of blank reactions was also carried out, in which the IPF solution along with urea was heated at the same temperature as that was used for nucleosides phosphorylation and phosphonylation reactions (55°C – 68°C). After the completion, a similar quenching protocol was followed and samples were analyzed by ^{31}P -NMR (SI Fig. S-10).

Reaction mixtures were quantified using an internal standard (0.1 M phosphonoacetic acid or PAA, hereafter). PAA was identified in the reaction sample as a triplet (H-coupled mode of ^{31}P -NMR) between 14 and 16 ppm with peaks that may shift due to changes in the pH (SI).

Reactivity Comparison of the Reduced Oxidation State P Compounds with Prebiotically Relevant Phosphate Minerals and Related Phosphites

Phosphate minerals such as apatites, vivianite, and brushite are likely to have existed in the Hadean and may be the most abundantly occurring prebiotic phosphate minerals (Keefe and Miller 1995; Schwartz 2006; Hazen et al. 2008; Burcar et al. 2019). In order to better understand the mechanism of the phosphorylation, the release of P from prebiotically relevant minerals including apatite, vivianite, and brushite and their relative reactivities with uridine were also studied. In addition, similar studies were also carried out with another P system comprising of a reduced oxidation state P compound; e.g., synthesized FeHPO_3 which represented a simple mineral phase of phosphite (HPO_3) $^{2-}$, which could be present on the early Earth. The synthesized FeHPO_3 was also catalyzed with H_2O_2 under similar conditions as (Pasek et al. 2008) to see whether the reaction is feasible with reduced oxidation state P minerals (i.e., synthesized FeHPO_3).

Mineralogy in Fenton Solutions

A 0.1 M solution of CaCl_2 was added dropwise to a glass beaker containing 7 mL of IPF solution at room temperature. White precipitates immediately formed, which were filtered, dried, and stored for laser Raman spectroscopic analysis. In a separate experiment, similar steps were repeated to study the effect of Mg^{2+} ions by adding 0.05–0.1 M anhydrous MgCl_2 solution dropwise to 7 mL of IPF solution. Once again thick white precipitates were observed which were filtered, dried at room temperature, and saved to be analyzed by Raman and XRD.

The precipitates started to form with concentrations as low as 0.05 M solution of the respective Ca^{2+} or Mg^{2+} ions, but the process was relatively slow and needed 24 h to 2 days of consistent stirring at room temperature. However, when 0.1 M solutions of the above-mentioned ions were used, white precipitates formed almost immediately.

Results

Prebiotic phosphorylation and phosphonylation reactions of the nucleosides were carried out by heating the organics with the inorganic P compounds generated via Fenton chemistry. The reactions produced organophosphites and organophosphates, including phosphate diesters via *one-pot syntheses*. Furthermore, the plausible stability of adenosine nucleoside in an environment saturated with H_2O_2 was also investigated. In addition, the mineralogy of inorganic P compounds generated via Fenton chemistry was also studied.

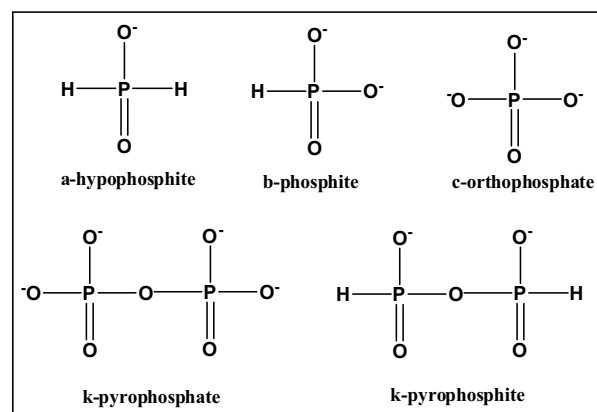
The Fenton reaction of the reduced oxidation state P compounds ($\text{NaH}_2\text{PO}_2 \cdot \text{H}_2\text{O}$) and FeHPO_3 produced orthophosphate and condensed P species when H_2O_2 was used in the molar concentration ranges of 0.1–0.5 M. Heating (at 55°C – 68°C) in the presence of urea specifically seemed to generate various inorganic condensed P species (SI, table S-2, Fig. S-10a and b). The species identified included pyrophosphate (identified as a singlet peak in the negative region, e.g., -5.5 to -6.0 PPM of H-coupled ^{31}P -NMR) and pyrophosphite (splitting into two triplets in the negative region, e.g., -3.5 to -6.5 PPM of H-coupled ^{31}P -NMR). In our studies, Fenton reaction of hypophosphite at the room temperature generated phosphite, orthophosphate, pyrophosphate and heating in the presence of urea also produced pyrophosphite.

Heating uridine, adenosine and 2'-deoxyadenosine with the IPF solution produced organophosphites and organophosphates (Table 1 and Figs. 1, 2, 3, and 4; SI Tables S-1–3 and Figs. S-2–9). The phosphorylated products of the reactions (i.e., uridine monophosphates, adenosine monophosphates) were identified by spiking with authentic standards (green arrowheads in each figure show the location of the

Table 1 ^{31}P -NMR relative abundances (%) of the phosphorus compounds detected in the reaction mixture of uridine and reduced oxidation phosphorus compounds

Sample name	hypophosphite	phosphite	orthophosphate	5'-mono- PO_3	5'-mono- PO_4	2'-or 3'-mono- PO_3	2'-or 3'-mono- PO_4	organic dimer	2',3'-cyclic mono- PO_4	Pyrophosphate and Pyrophosphite	Total Org. PO_3	Total Org. PO_4	^{13}C -O-P
	a	b	c	d	e	f	g	h	i	k			
Y2	27	14	17	17	3	13	1	2	5	2	31	11	42
238	16	10	1	24	15	24	5	ND	2	3	47	22	69
Ur2	20	ND	2	17	8	25	12	2	14	ND	42	36	78
Ad1	13	37	19	7	5	3	ND	ND	4	ND	10	9	19
Ad2	13	9	2	22	6	17	4	5	22	ND	39	37	76
Ur4	21	10	1	8	13	17	5	5	20	ND	25	43	68
D-ad	23	38	10	6	7	1	8	ND	ND	7	7	15	22
239	12	51	29	3	2	2	1	ND	ND	ND	5	3	8
HE3	–	9	58	ND	13	ND	4	ND	ND	16	ND	17	17

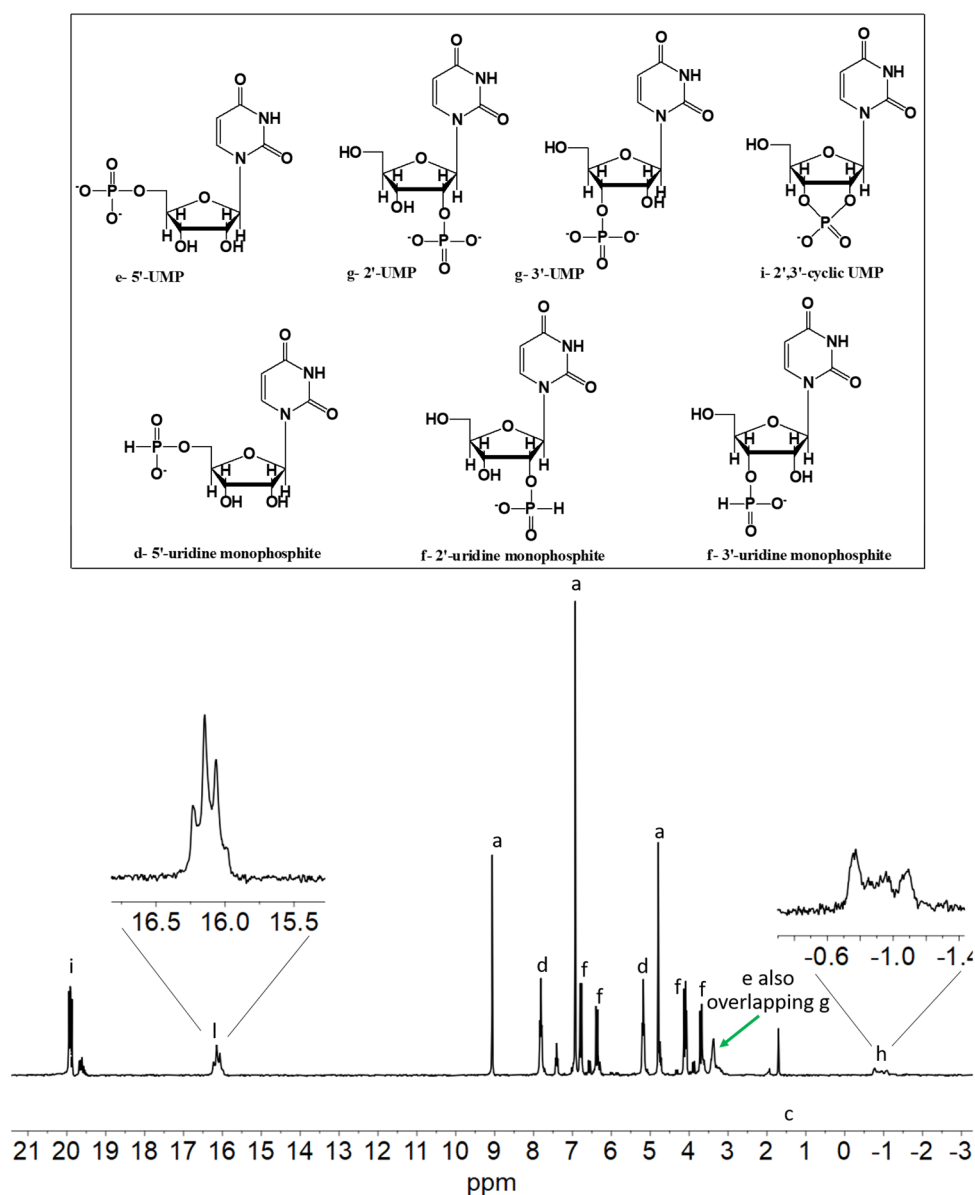
¹The relative abundances (%) of the phosphorylated products as well as other inorganic phosphates were calculated on the basis of the total phosphorus dissolved and by the peak integration method as previously reported (Gull et al. 2020). ^{13}C -O-P means total C-O-P (carbon-oxygen-phosphorus) type organic-P compounds, e.g., sum of organic phosphates and phosphites for that particular reaction (and may not be the exact sum due to rounding). Various products and their respective structures are identified as follows; a: hypophosphite, b: inorganic phosphite, c: inorganic phosphate, d: 5'-organic phosphite, e: 5'-organic phosphate, f: 2' or 3'-organic phosphite, g: 2' or 3'-organic phosphate, h: organic dimer species (U-P-U or Ad-P-Ad), i: 2',3'-cyclic monophosphate, (k): inorganic P species including condensed phosphates or phosphites. ND means not detected

**Fig. 1** Structures of inorganic P compounds discussed in the text: a-hypophosphite, b-phosphite, c-orthophosphate, k-condensed phosphates including both pyrophosphate and pyrophosphite, respectively. Labeling is consistent with the text and the ^{31}P -NMR figures

spiked peak), and looking at the nature and types of the peak splitting in the H-coupled NMR (e.g., singlet, triplet, and multiplets) and peak location (ppm). The formation of diesters consisting of uridine-phosphate-uridine and adenosine-phosphate-adenosine was identified in both ^{31}P -NMR and MS analyses. All the organic-P compounds bore only one P atom and no di- or tri-phosphates or phosphites were observed.

Figure 1 shows various inorganic P species discussed in the text while Fig. 2 shows the uridine reaction with the Fenton solution (also see SI Figs. S-2–7). Similar reaction trends were also seen with the nucleoside adenosine (SI Figs. S-8 and 9). Heating adenosine with the IPF solution and urea produced various adenosine phosphates and phosphites (Fig. 3). The major compounds were identified by spiking with standard compounds (SI Fig. S-9a and b). Figure 3 shows the various P species without any spiking with standard compounds while Fig. S-9a and b (SI) show the reaction solution spiked with authentic compounds including 2',3'-cyclic AMP, 3',5'-cyclic AMP (SI Fig. S-9a) and 5'-AMP (SI Fig. S-9b), respectively. The peak around – 2 ppm represents the standard compound 3',5'-cyclic AMP (SI Fig. S-9a). This peak is absent in the Fig. 3 (^{31}P -NMR without any spiking with authentic compound) indicating that this compound is not present in the reaction mixture. The peak around 20 ppm matches with the standard 2',3'-cyclic AMP (peak i) (SI Fig. S-9b) indicating the presence of this compound in the reaction solution. Figure S-9a (SI) shows the same reaction solution spiked with 5'-AMP (peak e). Figure 3 also shows a triplet (peak l) between 14 and 16 ppm for the internal standard (0.1 M phosphonoacetic acid or PAA). The peak l in Fig. S-9a and b (SI), is slightly shifted due to changes in the pH of the solutions.

Fig. 2 H-coupled, ^{31}P -NMR of Phosphorylation and phosphonylation reactions of uridine (sample Ur2). The labeled peaks correspond to the following compounds; a: sodium hypophosphite, b: inorganic phosphite, c: inorganic orthophosphate, d: 5'-uridine phosphite, e: 5'-UMP, f: 2'- and 3'-uridine phosphites, g: 2'- and 3'-UMP, h: organic dimer species (U-P-U), i: 2',3'-cyclic UMP, peaks k (inorganic condensed P compounds although not detected here) and peak l: internal standard phosphonoacetic acid (PAA)

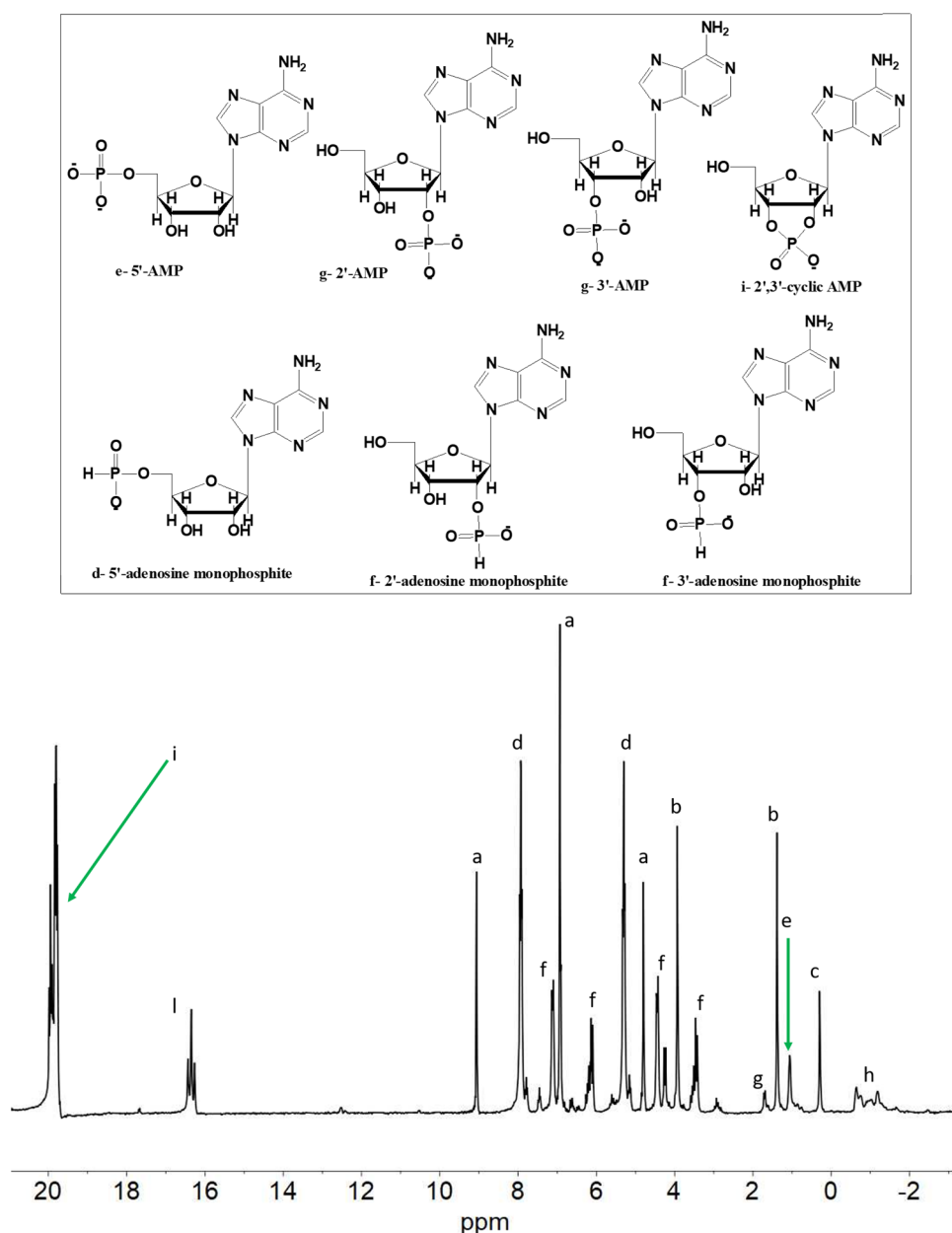


The NMR peak identifications were also confirmed by MS by the direct injection method as previously (Gull et al. 2020) (SI Figs. S-11–13). For the solutions with uridine we observed: $[\text{C}_9\text{N}_2\text{O}_6\text{H}_{11}\text{-H}]$ at m/z 243 corresponding to uridine nucleoside, $[\text{C}_9\text{N}_2\text{O}_9\text{PH}_{13}\text{-H}]$ at m/z 323.04 corresponding to uridine-monophosphate (2', 3' as well as 5'-UMP, respectively), $[\text{C}_9\text{H}_{11}\text{N}_2\text{O}_8\text{P-H}]$ at m/z 305.0 corresponding to 2',3'-cyclic UMP, $[\text{C}_9\text{N}_2\text{O}_8\text{PH}_{12}\text{-H}]$ at m/z 307 corresponding to uridine-monophosphite and finally, $[\text{C}_{18}\text{N}_4\text{O}_{14}\text{PH}_{23}\text{-H}]$ at m/z 549 represented the dimer species uridine-phosphate-uridine (U-P-U). The diester U-P-U was likely formed when uridine-monophosphate was condensed with another uridine unit with the loss of one water molecule. The diester molecule was identified by its location around -1 ppm region of ^{31}P -NMR spectrum and also by

the multiplicity (i.e., a multiplet of the peaks when H-coupled (Gull et al. 2020).

Similarly, the key peaks via MS were identified for the adenosine reaction in the Fenton solution. For the solutions with adenosine we observed: $[\text{C}_{10}\text{H}_{13}\text{N}_5\text{O}_4\text{-H}]$ at m/z 266 corresponding to adenosine nucleoside, $[\text{C}_{10}\text{H}_{13}\text{N}_5\text{O}_7\text{P-H}]$ at m/z 346 corresponding to monophosphate (2', 3' as well as 5'-AMP respectively), $[\text{C}_{10}\text{H}_{14}\text{N}_5\text{O}_6\text{P-H}]$ at m/z 330 corresponding to adenosine-monophosphite and finally, $[\text{C}_{20}\text{H}_{25}\text{N}_{10}\text{O}_{10}\text{P-H}]$ at m/z 595 represented the dimer species adenosine-phosphate-adenosine (Ad-P-Ad) (SI Figs. S-14–16). The diester was observed by ^{31}P -NMR, based on the location of the characteristic peak around -1 ppm and the pattern of the spin multiplicity in the H-coupled

Fig. 3 H-coupled ^{31}P -NMR of phosphorylation and phosphonylation reactions of adenosine (sample Ad2): Fig. 3 represents the reaction solution with added internal standard (0.1 M phosphonoacetic acid). The labeled peaks represent the following compounds; a: sodium hypophosphite, b: inorganic phosphite, c: inorganic orthophosphate, d: 5'-adenosine phosphite, e: 5'-AMP, f: 2' and 3'-adenosine phosphites, g: 2' and 3'-UMP, h: organic dimer species (A-P-A), i: 2',3'-cyclic AMP, k: inorganic condensed P compounds (not detected here), l: internal standard phosphonoacetic acid



mode. However, the exact structure of the isomer was not determined.

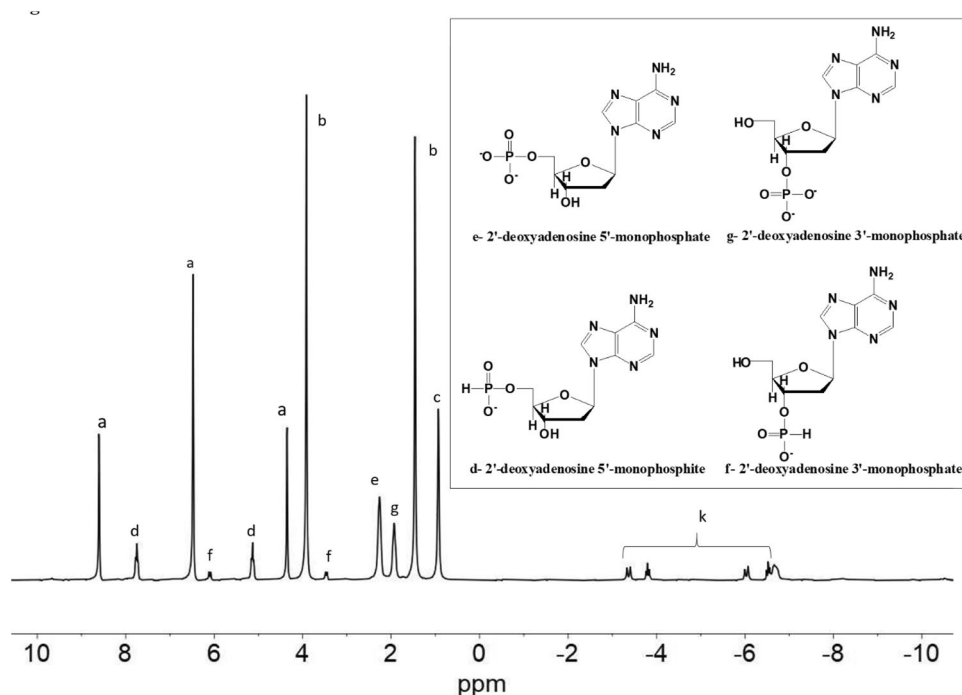
The optimum pH range suitable for one-pot phosphonylation and phosphorylation was found to be 7–9, and the most suitable temperature range was 55 °C–68 °C, although C–O–P products could also be seen around 68 °C–70 °C.

The uridine nucleoside reactions were found to be temperature- and time-sensitive, implying that prolonged heating would also cause rapid decomposition of uridine (seen as brownish to dark tar). In the case of uridine, the best reaction (Fig. 2; Table 1: sample Ur2) was observed when the reaction was carried out at the lower temperature of 55–60 °C for 2 days. Also, this reaction was further facilitated by NH_4OH and urea, resulting in a total relative abundance of

the C–O–P type compounds to be around 78% compared to other reactions (Table 1, Tables S-1–3). The yields (%) for this reaction, based on the internal standard and with respect to the quantity of phosphorus compounds used (i.e., the limiting reagent), were as follows: 2'-UMP and 3'-UMP combined yields (5%), 5'-UMP (3%), 2',3'-cyclic UMP (6%), uridine-phosphate-uridine (U-P-U) (1%), 2' and 3'-uridine-monophosphite (10%), 5'-uridine-monophosphite (7%), with a total yield of uridine phosphites and phosphates to be around 32%, respectively.

The adenosine nucleoside provided the highest relative abundance of the C–O–P type compounds (77%) when heated at the relatively higher temperature window (60–68 °C) for 3 days (Fig. 3, Table 1: sample Ad2). As also

Fig. 4 H-coupled ^{31}P -NMR of Phosphorylation and phosphonylation reactions of deoxyadenosine (sample D-Ad). The labeled peaks represent the following compounds; a: sodium hypophosphite, b: inorganic phosphite, c: inorganic orthophosphate, d: 5'-deoxyadenosine phosphite, e: 5'-deoxyadenosine monophosphate, f: 3'-deoxyadenosine phosphites, g: 3'-deoxyadenosine monophosphate, k: condensed inorganic P species, with some structures provided in the inset



seen in the uridine phosphonylation and phosphorylation reactions, the reactions were catalyzed by NH_4OH and urea. The yields (%) for this reaction, based on the internal standard, were as follows: 2'-AMP and 3'-AMP combined yields (1.5%), 5'-AMP (2%), 2',3'-cyclic AMP (11.5%), adenosine-phosphate-adenosine (A-P-A) (2.50%), 2' and 3'-adenosine-monophosphite (8%), 5'-adenosine-monophosphite (6%), with a total yield of adenosine phosphites and phosphates to be around 31.5%, respectively. Again, these yields are with respect to the total phosphorus added to the solution, which was the limiting reagent compared to the nucleoside substrate.

We also attempted the phosphorylation and phosphonylation of 2'-deoxyadenosine nucleoside (Fig. 4). Although the relative abundances were low compared to adenosine, the reactions did produce the respective nucleotide phosphite and phosphate esters. The reaction was temperature sensitive and was successful only in the temperature window of 55 °C–60 °C for two days heating. In this case no cyclic organic P nor P diesters were formed, implying: (1) diester formation is related to the formation of the cyclic organic monophosphates or (2) in our syntheses the consistent cyclic organic monophosphates were usually of the 2', 3'- type.

Because 2',3'-cyclic organophosphate compounds are not structurally possible in the case of 2'-deoxyadenosine, we conclude that formation of the dimer (both in case of uridine and adenosine) may require the 2'3'-cyclic nucleotide (Fig. 3).

In the comparative experimental study of the reactivities and P release by various prebiotically relevant minerals (e.g.,

brushite, vivianite, and apatite) with a Fenton system consisting of $\text{FeHPO}_3/\text{H}_2\text{O}_2$ (SI Table S-3 (reaction sample HE3, (Fig. 5, SI S-6, S-17)), it was found that the aqueous solution containing vivianite or apatite mineral did not release any phosphate, implying that the only P source would come from iron phosphite solution added to the round bottom flask along with uridine. As expected, the ^{31}P -NMR suggested the presence of orthophosphate (relative abundance: 58%), which was the oxidation product of iron phosphite FeHPO_3 , catalyzed by H_2O_2 , and the total % of the relative abundance of uridine-monophosphates were observed to be around 17% with no detectable amount of uridine monophosphites, consistent with the ^{31}P -NMR results (Fig. 5, SI S-6, S-17). This suite of experiments suggested that the various P species generated by the Fenton reaction could incorporate into the organic compounds and produce a variety of various related phosphorylated and phosphonylated derivatives.

Furthermore, when uridine was directly heated with the unquenched Fenton reaction solution, the major products detected were uridine phosphites (with low yields, e.g., less than 1%). Although, the uridine phosphates were below detection limits, nevertheless, the presence of uridine phosphites indicated the feasibility and ease of formation of organic P esters via Fenton chemistry. However, such reactions were not efficient at these lower pH (around 4.5).

The decomposition reactions of adenosine nucleoside in a Fenton environment were also carried out in order to better understand the feasibility of phosphorylation and phosphonylation in the environments containing H_2O_2 (SI). The decomposition rates of a 0.18 M aqueous solution of

adenosine (also containing an aqueous solution of 0.05 M $\text{FeCl}_2 \cdot 4\text{H}_2\text{O}$) were studied over the course of four days. Samples were regularly withdrawn to study the decomposition of adenosine in the presence of H_2O_2 (see SI for details). It was observed that at 22 °C–25 °C, the nucleoside was somewhat stable in the Fenton environment for up to two days and on the third day it started decomposing. ^{13}C -NMR was used for the qualitative studies of the decomposition of adenosine nucleoside (SI Figures S-18a–d). Figure S-18a shows the ^{13}C -NMR of the pure adenosine which can be compared with the chemical database (John Wiley & Sons, Inc. SpectraBase). LCMS studies that were employed for the quantitative analyses, revealed that the amount of adenosine in an environment containing H_2O_2 decreases over time (Fig. 6). Even though the decomposition rates were fast, this time window (2–4 days) may still be sufficient for phosphorylation and phosphonylation to occur.

When the IPF Solution (around pH 9–10) was treated with a 0.05–0.1 M anhydrous CaCl_2 solution, a white precipitate formed immediately. This precipitate was identified through Raman spectroscopic analysis to be brushite ($\text{CaHPO}_4 \cdot 2\text{H}_2\text{O}$) (Fig. 7). The peaks at 1000 cm^{-1} and 1066 cm^{-1} indicated the presence of phosphite and, in the presence of Ca^{2+} , would be CaHPO_3 (Fig. 7). Furthermore, XRD studies also confirmed that the white precipitate is brushite (Fig. 8). The sample (represented in black color) XRD pattern has a major peak at $12^\circ(2\theta)$ and a small peak at $20.5^\circ(2\theta)$, which is in agreement with pure brushite minerals (sample diffractogram Fig. 8).

When aqueous solution of MgCl_2 was slowly added to IPF Solution (already saturated with NH_4OH) at pH = 9, white precipitates were observed once again. The Raman spectrum of the white precipitates show two major peaks (947 cm^{-1} and 1000 cm^{-1} , blue line), which are consistent with struvite ($\text{NH}_4\text{MgPO}_4 \cdot 6\text{H}_2\text{O}$) (947 cm^{-1} , black line) and heterosite (FePO_4) (1001 cm^{-1} , red line) (Fig. 9). The

presence of struvite in this white precipitate was also confirmed by powder XRD analysis (Fig. 10).

An H–O–P Pourbaix diagram (Fig. 11) (Eh–pH, hereafter) was constructed to check the feasibility of the formation of struvite and brushite at pH = 9–10 from a solution possibly containing various inorganic P species (i.e., $(\text{H}_2\text{PO}_2)^-$, $(\text{PO}_4)^{3-}$, $(\text{HPO}_3)^{2-}$). The Eh–pH diagram predicts the occurrence of hydrogen phosphate ions at the given pH (Pasek 2008). This suggests that when Ca^{2+} ions are added into the Fenton solution at pH 9–10, the most plausible calcium-phosphorus compounds are expected to be CaHPO_3 , and CaHPO_4 , respectively, supporting the idea that the white precipitates are indeed a mixture of CaHPO_3 , and CaHPO_4 , while remains CaH_2PO_2 water soluble (Pasek 2008).

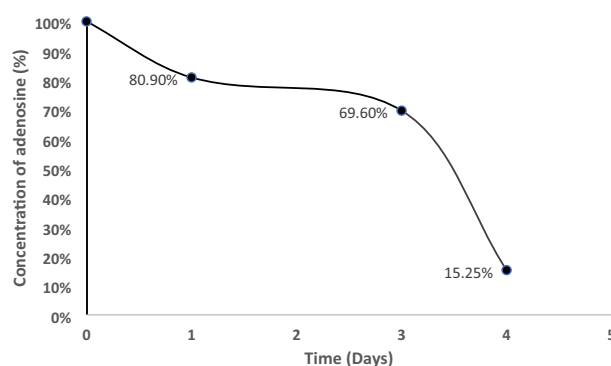


Fig. 6 Decomposition reactions of adenosine in an environment saturated with H_2O_2 (at 22–25 °C and pH = 3). Concentration of adenosine was calculated over the course of four days. The decomposition reactions were studied by slowly adding (over the course of 4 days) an aqueous solution of 0.5 M H_2O_2 to an aqueous solution mixture of 0.18 M adenosine and 0.05 M $\text{FeCl}_2 \cdot 4\text{H}_2\text{O}$, respectively

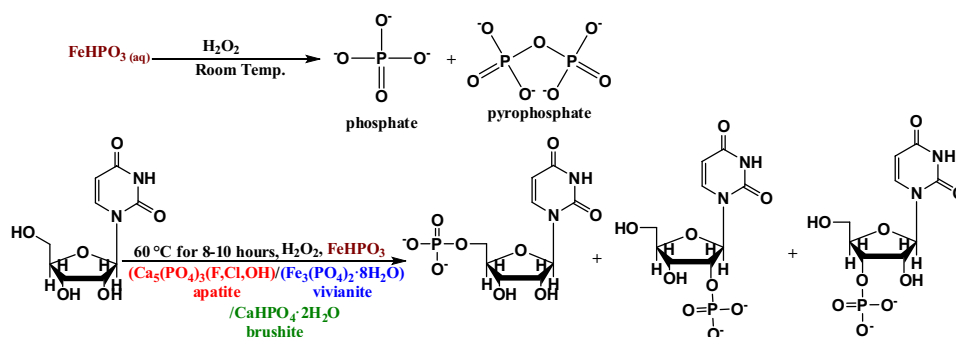


Fig. 5 Reactions to compare the release of phosphorus from various mineral sources and its reactivity with the uridine nucleoside under early Earth conditions. The reactivity of the phosphate minerals (apatite, vivianite, and brushite) was compared with that of the phosphate released by the Fenton reaction of FeHPO_3 , a simple mineral phase of

iron. Various minerals are shown in different colors. The major products included 5'-UMP along with 2' or 3'-UMP. In the first step of the Fenton reaction, FeHPO_3 produces phosphate and pyrophosphate at room temperature followed by the phosphorylation and phosphonylation

Discussion

The reaction of inorganic-P molecules generated via Fenton chemistry with uridine and adenosine demonstrates that reduced P compounds bear an increased reactivity compared to phosphates and may have enabled biomolecule formation on the early Earth (Fig. 12). Modern life requires RNA, built from activated nucleotides and a P source and performing key roles in the metabolic processes of modern life. Phosphorylation on the early Earth would have played a pivotal role in the chemical milieu, generating organophosphate biomolecules essential to life through the oxidation of reduced P compounds. The proposed reaction series would require an environment that produces both soluble iron and reduced P compounds as a first step. Given that iron (Fe^{2+}) is capable of producing reduced P from phosphate (Hersch et al. 2018), a pool bearing both reduced P and Fe^{2+} should be feasible.

A plausible site for the proposed phosphorylation and phosphonylations would be a mildly hot drying alkaline pond. The hot temperatures and alkaline pH are seen in the present day at the Lost City hydrothermal fields in the mid-Atlantic Ocean with pH = 9–10 and temperatures ranging from 40 °C to 75 °C (Kelley et al. 2001, 2005; Fröh-Green et al. 2003). A small associated pond linked up with such environments could have concentrated organics and the necessary P compounds to kickstart such reactions. Furthermore, this Fenton chemistry is likely to have existed on rocky planets including the early Earth (Pasek et al. 2008).

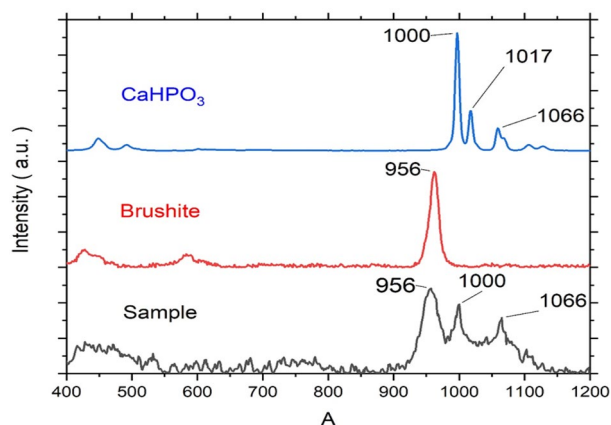


Fig. 7 Raman spectroscopic data of the sample (white precipitates formed by adding anhydrous CaCl_2 solution to IPF solution) compared with the synthesized calcium phosphite and RRUFF's data. Starting from bottom to top: black colored spectrum is that of the sample (white precipitates) while the red colored spectrum is that of standard brushite mineral as derived from RRUFF database (R070554; RRUFF database) and blue spectrum is that of pure synthesized calcium phosphite (Color figure online)

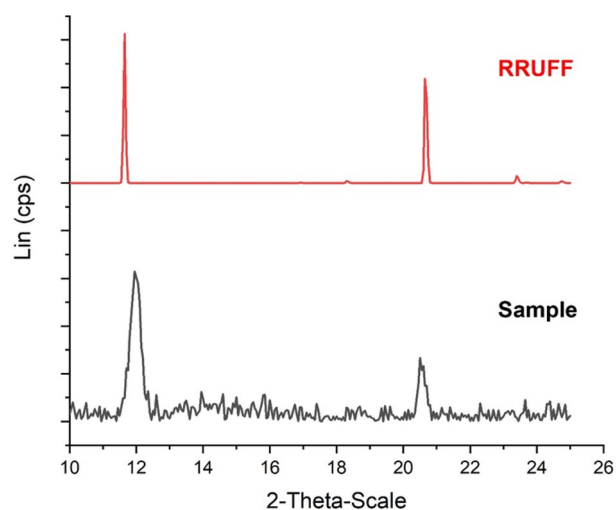


Fig. 8 Powder X-Ray Diffraction patterns of the white precipitates obtained by adding aqueous solution of anhydrous CaCl_2 to IPF solution (black colored diffractogram) compared with the standard diffractometry patterns taken from RRUFF database (red line, brushite, RRUFF ID: R070554) (Color figure online)

It is possible that during the early Earth's history, a Snowball Earth event would have produced enough H_2O_2 to leave a global fingerprint. Furthermore, during a Snowball event, the circulation of the ocean waters through the hydrothermal systems would have built up higher concentration of metals such as Fe^{2+} and Mn^{2+} (Liang et al. 2006). Although the severity of such historical events is

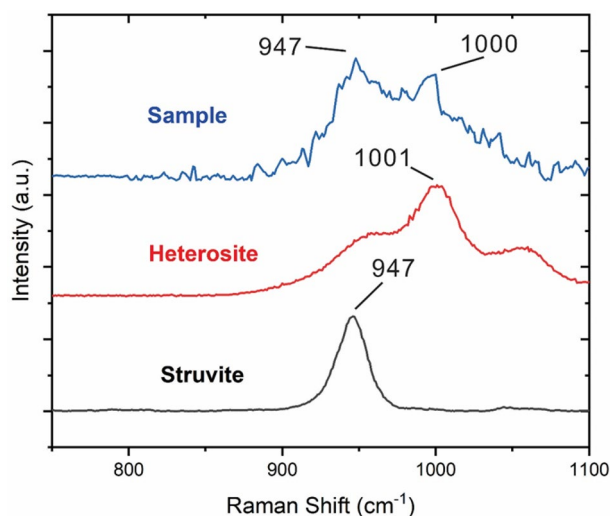


Fig. 9 Raman analysis for sample product (white precipitates formed by adding MgCl_2 solution (blue line) to IPF solution) with comparison to the spectroscopic standards from the RRUFF database (black line, struvite, RRUFF ID: R050511; red line, heterosite, RRUFF ID: 050,165) (Color figure online)

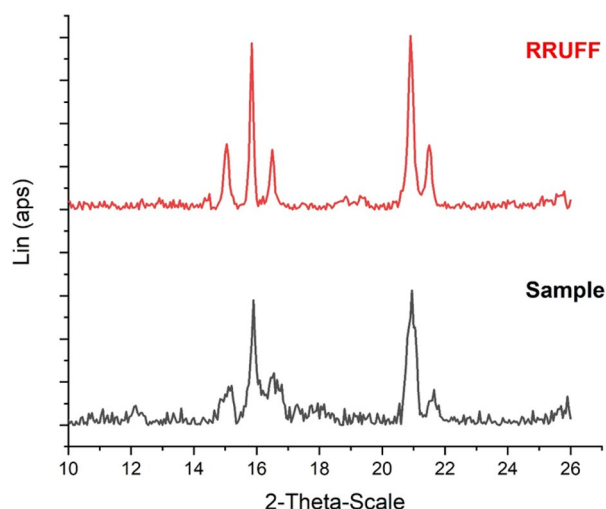


Fig. 10 Powder X-Ray Diffraction patterns for sample product for Fenton solution reaction with ammonia and MgCl_2 (black line) with comparison to the diffractometry standards from RRUFF database (red line, struvite, RRUFF ID: R050511) (Color figure online)

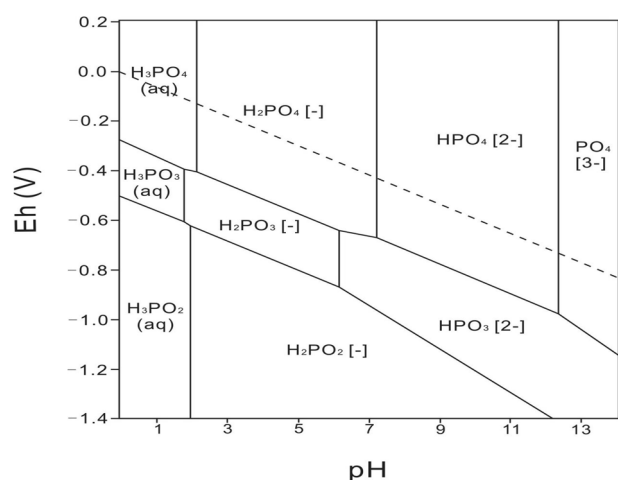


Fig. 11 H–O–P Pourbaix diagram showing the feasibility of the formation of struvite and brushite at $\text{pH}=9.5\text{--}10$ from a solution possibly containing various inorganic P species, i.e., $(\text{H}_2\text{PO}_2)^-$, $(\text{PO}_4)^{3-}$, $(\text{HPO}_3)^{2-}$, respectively

still questioned, such “hard Snowball” events would have resulted in a weak hydrological cycle that would have provided a sustained production of H_2O_2 when coupled with the photochemical reactions involving water vapor (Liang et al. 2006).

Hence, it is plausible that under such geological conditions, a variety of inorganic P compounds would have generated via Fenton chemistry in the presence of H_2O_2 and Fe^{2+} (Pasek et al. 2008) that later on would have been able to phosphorylate (and phosphonylate) the organics under mild heating conditions. While assuming all these reactions could

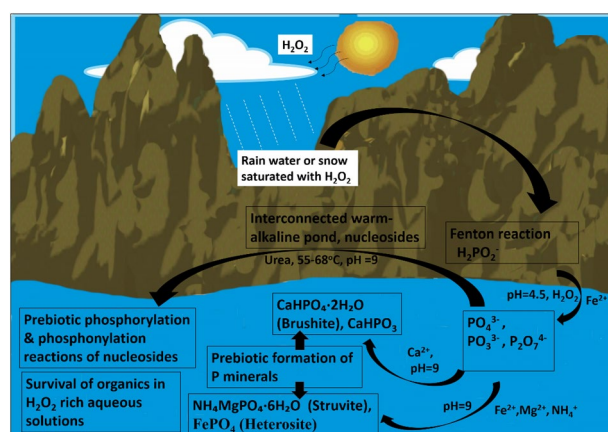


Fig. 12 Schematic illustration showing various prebiotic scenarios suggested in the text

be happening in a single pond might seem contrived, the idea of separate ponds interlinked by streams or heavy rain-falls to help in the mixing of multi-pot processes has been suggested by Clarke and Kolb (2020); Sutherland (2016); Ritson and colleagues (2018); and Damer and Deamer (2018, 2020).

We found that vivianite, brushite, and apatite did not release any detectable amount of P into in water (Burcar et al. 2019). Apatite has also shown to phosphorylate thymidine with considerable yields but only under harsh conditions requiring cyanides, ammonium compounds and heating at $90\text{ }^\circ\text{C}$, for extended periods of time (Schwartz et al. 1975).

In this study, the presence of ammonium compounds seemed to enhance the overall production of the phosphite and phosphate esters of nucleosides. The best yields in our setup were seen when the Fenton reaction mixture was quenched with NH_4OH in conjunction with urea as a condensation agent. The organic-P products could easily be detected after heating the reaction mixture at $65\text{ }^\circ\text{C}$ – $68\text{ }^\circ\text{C}$ for time periods as short as 1 day. The yields of organic phosphite and phosphate esters drastically declined when no ammonium source was added, and the Fenton reaction was quenched with NaOH solution but organic phosphites and phosphates remained detectable under all circumstances. This observation is in contrast to earlier findings in which the meteorite mineral schreibersite was used as a P source and could give detectable yields of nucleotides only in the presence of compounds including urea, K_2CO_3 or NH_4OH (Gull et al. 2015). The reactions presented here are comparable with previously reported ones (Handschuh et al. 1973; Pasek and Lauretta 2005; Pasek et al. 2007, 2013; Gull et al. 2015). Furthermore, the results are also comparable with the other previously reported work in which ammonium phosphite or $(\text{NH}_4)_2\text{HPO}_3$ was reacted with uridine at $60\text{ }^\circ\text{C}$ and within 24 h around 20% yield of uridine-5'-phosphite was

obtained. When a similar reaction was repeated in the presence of urea as a condensation agent, the yield was remarkably improved to be around 44% in 24 h (Graaf and Schwartz 2005).

In order to further understand the mechanism of the reaction, when the Fenton solution (IPF) was heated in the presence of urea (and with no other organic added), the ^{31}P -NMR studies revealed that it produced various inorganic P condensed species of phosphates and phosphites (SI Fig. S-10). These condensed species seemed to disappear in the absence of urea, suggesting that urea promotes such condensed P species which actively participated in the formation of phosphates and phosphites of nucleosides under such mild temperatures. This is suggestive that condensed phosphates such as pyrophosphate generated via Fenton chemistry may react with ammonium compounds and produce high-energy phosphates such as amidophosphates in solution that then phosphorylate organics, as demonstrated previously (Gibard et al. 2019). Both urea and NH_4OH are considered prebiotically relevant compounds (Lohrmann and Orgel 1968; Schwartz et al. 1975; Burcar et al. 2016, 2019; Gibard et al. 2019). Importantly, the P rich solution generated via the Fenton route yielded phosphodiester of uridine and adenosine that were likely formed via the opening of 2',3'-cyclic monophosphate. Phosphate diesters play a critical role in nature by acting as a molecular 'tape' that connects the individual nucleotides in DNA and RNA through a sugar-phosphate backbone. The present study also highlights a plausible route for the prebiotic syntheses of diester type derivatives of the nucleosides. However, the full characterization of the exact structure, and the stability of these diester derivatives of the nucleosides under (aqueous) Hadean conditions is unclear. The results in this paper are comparable with our previously reported studies (Gull et al. 2020) in which uridine reacted with pyrophosphate in the presence of Mg^{2+} and urea and yielded monoesters of uridine as well as a consistent presence of the U-P-U diester under all circumstances.

The discovery of H_2O_2 in the Martian environment (Clancy et al. 2004; Encrenaz et al. 2005; Ito et al. 2020) strongly suggested it to be one of the leading oxidizers on the Martian surface. This idea is strongly supported by the GC-MS studies on the Viking 1976 Mars missions that could not detect any organic compound on the Martian surface, even those expected from meteorite bombardment (Benner et al. 2000). Benner and colleagues have suggested certain metastable intermediates of meteoritic organics under such oxidizing conditions, e.g., nonvolatile salts of benzenecarboxylic acids, oxalic and acetic acid (Benner et al. 2000). They also suggested the plausibility of Fenton chemistry on the Martian surface (Benner et al. 2000). Organics have been detected on the Martian surface by the Mars rovers (Szopa et al. 2020; Millan et al. 2022; Steele et al. 2022). These organics could

still plausibly be the outcome of certain decomposition as suggested before (Benner et al. 2000).

Our study on the exposure of adenosine to harsh environments (Fenton solution and H_2O_2) question the longevity and stability of such organic compounds as also suggested by Benner and colleagues (2000). Further studies would require investigating the decomposition rates and the ultimate products of the organics exposed to such harsh conditions containing H_2O_2 . H_2O_2 has also been found on the surface of Europa (the icy moon of Jupiter) and phenomenon such as radiolysis and photolysis of its icy surface leads to the formation of oxygen and ROS (reactive oxygen species) (Ślesak et al. 2012). It is therefore highly likely that the early Earth as well as other rocky planets including Mars would have to face the harsh conditions including the presence of H_2O_2 . However, our results showing the successful phosphorylation and phosphonylation reactions of the nucleosides in the presence of Fenton solution suggest that under heating conditions H_2O_2 decomposes to H_2O and O_2 thus making these reactions feasible.

At ambient temperatures, on adding Ca^{2+} to the quenched Fenton solution (in the absence of nucleosides and heat), there was a rapid conversion of phosphite and phosphate into calcium phosphite (CaHPO_3) and brushite ($\text{CaHPO}_4 \cdot 2\text{H}_2\text{O}$). Geochemical models predicted that calcium precipitation reactions would be pH dependent and favored at high pH (Pasek 2020). Our observations support these models, showing that the leaching of CaHPO_3 from solution occurs at pH 9–10. This also demonstrates the conversion of less mobile phosphates (from Fenton solution) to the lower solubility phosphates (brushite) in the presence of Ca^{2+} ions. Moreover, these reduced oxidation state P compounds (including from other sources such as meteoritic mineral schreibersite) would have settled in the Hadean oceans and would have been caught in 'sinks' of calcium phosphates. Similar precipitation occurs when Mg^{2+} ions were added in a separate IPF solution under similar conditions. The Raman spectroscopy of the dried sample matched with that of the mineral struvite. These findings also support the formation of struvite mineral on the early Earth (Handschuh and Orgel 1973; Feng et al. 2021). Struvite is considered ephemeral on the earlier Earth environments (Feng et al. 2021) and its plausibility on the early Earth is questionable (Gull and Pasek 2013). The proposed suite of experiments highlights a plausible mechanism of formation of this mineral on the early Earth.

The present work shows the significance of the reduced P compounds (especially phosphite) and their ubiquity on the early Earth. The reduced oxidation state P compounds have been detected in meteoritic minerals (Pasek and Lauretta 2005; Pasek et al. 2007), in the Archean carbonates (Pasek et al. 2013), in fulgurites (Pasek and Block 2009), in hydrothermal systems (Pech et al. 2009), in natural water systems (Pasek et al. 2014; Van Mooy et al. 2015), and also by geochemical reduction of phosphate into phosphite (Herschly et al. 2018;

Ritson et al. 2020). These results are significant as P mainly occurs in the form of phosphates on the modern Earth, most abundantly and commonly as apatites. The reaction of these reduced compounds with strong but prebiotically plausible oxidants results in solutions “primed” for phosphorylation. Such conditions may be plausible beyond the earth as well, given the prevalence of H_2O_2 beyond the earth, and the several routes that have been identified to generating reduced P compounds.

Supplementary Information The online version contains supplementary material available at <https://doi.org/10.1007/s00239-022-10086-w>.

Acknowledgements This work was supported by NASA Exobiology program (80NSSC18K1288). This work has also been supported in part by University of South Florida Interdisciplinary NMR Facility, The Department of Chemistry and the College of Arts and Sciences, Tampa, Florida. The Chemical Purification Analysis and Screening Core Facility (CPAS) at University of South Florida have supported the mass spectrometry data analysis. This manuscript was greatly benefited from the useful discussions with Prof. Dr. Ram Krishnamurthy (Scripps Research Institute). Authors also acknowledge the help of Prof. Bill Baker, Prof. Laurent Calcul from USF Chemistry department, and Danny Lindsay with the various instrumental set-ups during the project. Maheen Gull is extremely grateful to her husband Ryan for help with the figures and graphical abstract of the paper and watching the kids so that the experiments could be finished on time. Thanks are also due to Andrew Stella-Vega for the helpful discussions about the manuscript. The authors also thank the anonymous reviewers for the helpful suggestions. Maheen Gull would also like to thank her mother in Pakistan for all the support and to her father and finally to her daughters Luna Faye and Nova Joy for the inspiration to do better.

Declarations

Conflict of interest No competing financial interests exist for any of the authors.

References

- Arrhenius G, Sales B, Mojzsis S, Lee T (1997) Entropy and charge in molecular evolution—the case of phosphate. *J Theor Biol* 187:503–522
- Benner SA, Devine KG, Matveeva LN, Powell DH (2000) The missing organic molecules on Mars. *Proc Natl Acad Sci U S A* 97:2425–2430
- Blankenship RE, Hartman H (1998) The origin and evolution of oxygenic photosynthesis. *Trends Biochem Sci* 23:94–97
- Burcar B, Pasek M, Gull M, Cafferty BJ, Velasco F, Hud NV, Menor-Salván C (2016) Darwin’s warm little pond: a one-pot reaction for prebiotic phosphorylation and the mobilization of phosphate from minerals in a urea-based solvent. *Angew Chem Int Ed Engl* 55:13249–13253
- Burcar B, Castañeda A, Lago J, Daniel M, Pasek MA, Hud NV, Menor-Salván C (2019) A stark contrast to modern Earth: phosphate mineral transformation and nucleoside phosphorylation in an Iron- and Cyanide-Rich early Earth scenario. *Angew Chem* 131:17137–17143
- Clancy RT, Sandor BJ, Moriarty-Schieven GH (2004) A measurement of the 362 GHz absorption line of Mars atmospheric H_2O_2 . *Icarus* 168:116–121
- Clark BC, Kolb VM (2020) Macroblont: cradle for the origin of life and creation of a biosphere. *Life* 10:278
- Cooper GW, Onwo WM, Cronin JR (1992) Alkyl phosphonic acids and sulfonic acids in the Murchison meteorite. *Geochim Cosmochim Acta* 56:4109–4115
- Damer B, Deamer D (2020) The hot spring hypothesis for an origin of life. *Astrobiology* 20:429–452
- De Graaf RM, Schwartz AW (2005) Thermal synthesis of nucleoside H-phosphonates under mild conditions. *Orig Life Evol Biosph* 35:1–10
- Deamer DW (2018) Assembling life: how can life begin on earth and other habitable planets? Oxford University Press, Oxford
- Encrenaz T, Bézard B, Owen T, Lebonnois S, Lefèvre F, Great-house T, Forget F (2005) Infrared imaging spectroscopy of Mars: H_2O mapping and determination of CO_2 isotopic ratios. *Icarus* 179:43–54
- Feng T, Lang C, Pasek MA (2019) The origin of blue coloration in a fulgurite from Marquette, Michigan. *Lithos* 342:288–294
- Feng T, Gull M, Omran A, Abbott-Lyon H, Pasek MA (2021) Evolution of ephemeral phosphate minerals on planetary environments. *ACS Earth Space Chem* 5:1647–1656
- Früh-Green GL, Kelley DS, Bernasconi SM, Karson JA, Ludwig KA, Butterfield DA, Proskurowski G (2003) 30,000 years of hydrothermal activity at the Lost City vent field. *Science* 301:495–498
- Gibard C, Gorrell IB, Jiménez EI, Kee TP, Pasek MA, Krishnamurthy R (2019) Geochemical sources and availability of amidophosphates on the early Earth. *Angew Chem* 131:8235–8239
- Gilbert W (1986) Origin of life: the RNA world. *Nature* 319:618–618
- Gulick A (1955) Phosphorus as a factor in the origin of life. *Am Sci* 43:479–489
- Gull M (2014) Prebiotic phosphorylation reactions on the early Earth. *Challenges* 5:193–212
- Gull M, Pasek MA (2013) Is struvite a prebiotic mineral? *Life* 3:321–330
- Gull M, Zhou M, Fernández FM, Pasek MA (2014) Prebiotic phosphate ester syntheses in a deep eutectic solvent. *J Mol Evol* 78:109–117
- Gull M, Mojica MA, Fernández FM, Gaul DA, Orlando TM, Liotta CL, Pasek MA (2015) Nucleoside phosphorylation by the mineral schreibersite. *Sci Rep* 5:1–6
- Gull M, Cafferty BJ, Hud NV, Pasek MA (2017) Silicate-promoted phosphorylation of glycerol in non-aqueous solvents: a prebiotically plausible route to organophosphates. *Life* 7:29
- Gull M, Omran A, Feng T, Pasek MA (2020) Silicate-, magnesium ion-, and urea-induced prebiotic phosphorylation of uridine via pyrophosphate; revisiting the hot drying water pool scenario. *Life* 10:122
- Handsuh GJ, Orgel LE (1973) Struvite and prebiotic phosphorylation. *Science* 179:483–484
- Handsuh GJ, Lohrmann R, Orgel LE (1973) The effect of Mg^{2+} and Ca^{2+} on urea-catalyzed phosphorylation reactions. *J Mol Evol* 2:251–262
- Hazen RM, Papineau D, Bleeker W, Downs RT, Ferry JM, McCoy TJ, Yang H (2008) Mineral evolution. *Am Mineral* 93:1693–1720
- He H, Wu X, Xian H, Zhu J, Yang Y, Lv Y, Konhauser KO (2021) An abiotic source of Archean hydrogen peroxide and oxygen that pre-dates oxygenic photosynthesis. *Nat Commun* 12:1–9
- Herschby B, Chang SJ, Blake R, Lepland A, Abbott-Lyon H, Sampson J, Pasek MA (2018) Archean phosphorus liberation induced by iron redox geochemistry. *Nat Commun* 9:1–7
- Holm G (2012) The significance of Mg in prebiotic geochemistry. *Geobiology* 10:269–279
- Hud NV, Cafferty BJ, Krishnamurthy R, Williams LD (2013) The origin of RNA and “my grandfather’s axe.” *Chem Biol* 20:466–474
- Ito Y, Hashimoto GL, Takahashi YO, Ishiwatari M, Kuramoto K (2020) H_2O_2 -induced greenhouse warming on oxidized early Mars. *Astrophys J* 893:168

- John Wiley & Sons, Inc. SpectraBase; SpectraBase Compound ID=Bd8zMd0IP9g SpectraBase Spectrum ID=8tYWDqwGwxD, <https://spectrabase.com/spectrum/8tYWDqwGwxD> (Accessed 31/8/2022).
- Keefe AD, Miller SL (1995) Are polyphosphates or phosphate esters prebiotic reagents? *J Mol Evol* 41:693–702
- Kelley DS, Karson JA, Blackman DK, Früh-Green GL, Butterfield DA, Lilley MD, Rivizzigno P (2001) An off-axis hydrothermal vent field near the Mid-Atlantic Ridge at 30 N. *Nature* 412:145–149
- Kelley DS, Karson JA, Früh-Green GL, Yoerger DR, Shank TM, Butterfield DA, Sylva SP (2005) A serpentinite-hosted ecosystem: the lost city hydrothermal field. *Science* 307:1428–1434
- Laetsch T, Downs R (2006) Software for identification and refinement of cell parameters from powder diffraction data of minerals using the RRUFF Project and American Mineralogist Crystal Structure Databases. In 19th General Meeting of the International Mineralogical Association, Kobe, pp 28
- Lafuente B, Downs RT, Yang H, Stone N (2015) The power of databases: The RRUFF project. In: Armbruster T, Danisi RM (eds) Highlights in mineralogical crystallography. De Gruyter, Berlin, pp 1–30
- Lago JL, Burcar BT, Hud NV, Febrian R, Mehta C, Bracher PJ, Pasek MA (2020) The prebiotic provenance of semi-aqueous solvents. *Orig Life Evol Biosph* 50:1–14
- Lalonde SV, Konhauser KO (2015) Benthic perspective on Earth's oldest evidence for oxygenic photosynthesis. *Proc Natl Acad Sci U S A* 112:995–1000
- Levine JS, Hays PB, Walker JC (1979) The evolution and variability of atmospheric ozone over geological time. *Icarus* 39:295–309
- Liang MC, Hartman H, Kopp RE, Kirschvink JL, Yung YL (2006) Production of hydrogen peroxide in the atmosphere of a Snowball Earth and the origin of oxygenic photosynthesis. *Proc Natl Acad Sci U S A* 103:18896–18899
- Lohrmann R, Orgel LE (1968) Prebiotic synthesis: phosphorylation in aqueous solution. *Science* 161:64–66
- Millan M, Teinturier S, Malespin CA, Bonnet JY, Buch A, Dworkin JP, Mahaffy PR (2022) Organic molecules revealed in Mars's Bagnold Dunes by Curiosity's derivatization experiment. *Nat Astron* 6:129–140
- Olson JM (1970) The Evolution of Photosynthesis: Hypothesis: photosynthetic bacteria and blue-green algae shared a common photoheterotrophic ancestor. *Science* 168:438–446
- Padan E (1979) Facultative anoxygenic photosynthesis in cyanobacteria. *Annu Rev Plant Physiol* 30:27–40
- Pasek MA (2008) Rethinking early Earth phosphorus geochemistry. *Proc Natl Acad Sci U S A* 105:853–858
- Pasek MA (2019) Thermodynamics of prebiotic phosphorylation. *Chem Rev* 120:4690–4706
- Pasek M, Block K (2009) Lightning-induced reduction of phosphorus oxidation state. *Nat Geosci* 2:553–556
- Pasek MA, Kee TP (2011) On the origin of phosphorylated biomolecules. *Origins of life: the primal self-organization*. Springer, Berlin, Heidelberg, pp 57–84
- Pasek MA, Lauretta DS (2005) Aqueous corrosion of phosphide minerals from iron meteorites: a highly reactive source of prebiotic phosphorus on the surface of the early Earth. *Astrobiology* 5:515–535
- Pasek MA, Pasek VD (2018) The forensics of fulgurite formation. *Mineral Petrol* 112:185–198
- Pasek MA, Dworkin JP, Lauretta DS (2007) A radical pathway for organic phosphorylation during schreibersite corrosion with implications for the origin of life. *Geochim Cosmochim Acta* 71:1721–1736
- Pasek MA, Kee TP, Bryant DE, Pavlov AA, Lunine JI (2008) Production of potentially prebiotic condensed phosphates by phosphorus redox chemistry. *Angew Chem Int Ed Engl* 47:7918–7920
- Pasek MA, Harnmeijer JP, Buick R, Gull M, Atlas Z (2013) Evidence for reactive reduced phosphorus species in the early Archean ocean. *Proc Natl Acad Sci U S A* 110:10089–10094
- Pasek MA, Sampson JM, Atlas Z (2014) Redox chemistry in the phosphorus biogeochemical cycle. *Proc Natl Acad Sci U S A* 111:15468–15473
- Pasek MA, Gull M, Herschy B (2017) Phosphorylation on the early earth. *Chem Geol* 475:149–170
- Pech H, Henry A, Khachikian CS, Salmassi TM, Hanraha G, Foster KL (2009) Detection of geothermal phosphite using high-performance liquid chromatography. *Environ Sci Technol* 43:7671–7675
- Raymond J, Blankenship RE (2008) The origin of the oxygen-evolving complex. *Coord Chem Rev* 252:377–383
- Ritson DJ, Battilocchio C, Ley SV, Sutherland JD (2018) Mimicking the surface and prebiotic chemistry of early Earth using flow chemistry. *Nat Commun* 9:1–10
- Ritson DJ, Mojzsis SJ, Sutherland J (2020) Supply of phosphate to early Earth by photogeochemistry after meteoritic weathering. *Nat Geosci* 13:344–348
- Saladino R, Crestini C, Pino S, Costanzo G, Di Mauro E (2012) Formamide and the origin of life. *Phys Life Rev* 9:84–104
- Schoffstall AM (1976) Prebiotic phosphorylation of nucleosides in formamide. *Orig Life* 7:399–412
- Schwartz AW (2006) Phosphorus in prebiotic chemistry. *Philos Trans R Soc Lond B Biol Sci* 361:1743–1749
- Schwartz AW, Veen MV, Bisseling T, Chittenden GJ (1975) Prebiotic nucleotide synthesis-demonstration of a geologically plausible pathway. *Orig Life* 6(1–2):163–168. <https://doi.org/10.1007/BF01372401>
- Simonson BM, Glass BP (2004) Spherule layers—records of ancient impacts. *Annu Rev Earth Planet Sci* 32:329
- Simonson BM, Davies D, Wallace M, Reeves S, Hassler SW (1998) Iridium anomaly but no shocked quartz from Late Archean microkrystite layer: Oceanic impact ejecta? *Geology* 26:195–198
- Ślesak I, Ślesak H, Kruk J (2012) Oxygen and hydrogen peroxide in the early evolution of life on earth: in silico comparative analysis of biochemical pathways. *Astrobiology* 12:775–784
- Steele A, Benning LG, Wirth R, Schreiber A, Araki T, McCubbin FM, Rogers K (2022) Organic synthesis associated with serpentinization and carbonation on early Mars. *Science* 375:172–177
- Sutherland JD (2016) The origin of life—out of the blue. *Angew Chem Int Ed Engl* 55:104–121
- Szopa C, Freissinet C, Glavin DP, Millan M, Buch A, Franz HB, Cabane M (2020) First detections of dichlorobenzene isomers and trichloromethylpropane from organic matter indigenous to Mars mudstone in Gale Crater, Mars: results from the sample analysis at Mars instrument onboard the curiosity rover. *Astrobiology* 20:292–306
- Van Mooy BAS, Krupke A, Dyhrman ST, Fredricks HF, Frischkorn KR, Ossolinski JE, Sylva SP (2015) Major role of planktonic phosphate reduction in the marine phosphorus redox cycle. *Science* 348:783–785

Springer Nature or its licensor (e.g. a society or other partner) holds exclusive rights to this article under a publishing agreement with the author(s) or other rightsholder(s); author self-archiving of the accepted manuscript version of this article is solely governed by the terms of such publishing agreement and applicable law.

Authors and Affiliations

Maheen Gull¹ · Tian Feng¹ · Joe Bracegirdle² · Heather Abbott-Lyon³ · Matthew A. Pasek¹

✉ Maheen Gull
ambermaheen@yahoo.com

✉ Matthew A. Pasek
mpasek@usf.edu

² Department of Chemistry, University of South Florida,
Tampa, FL 33620-5250, USA

³ Department of Chemistry and Biochemistry, Kennesaw State
University, 370 Paulding Ave NW, Kennesaw, GA 30144,
USA

¹ School of Geosciences, University of South Florida, 4202 E
Fowler Ave., NES 204, Tampa, FL 33620, USA